Fengjun Shi[1,*], Hang Su[1], Lei Zhao[2], Xiuyan Yu[3], Shengxian Li[3]

[1] North China University of Water Resources and Electric Power, Zhengzhou, Henan 450045, China, * e-mail: shifengjun1962@126.com

[2] Dengdian Basalt Fibre Co. Ltd of Henan, Xingzheng, Henan 451100, China

[3] Textile Products Quality Supervision & Inspection Institute of Henan, Zhengzhou, Henan 450042, China

Study on the Structure and Properties of Continuous Basalt Fibres

DOI: 10.5604/01.3001.0014.0934

Abstract

The chemical composition, X-ray diffraction, thermal properties, flammability, mechanical properties and morphology of basalt fibres are investigated in this paper. Chemical analysis and energy dispersive X-ray fluorescence spectrometer experiments showed that basalt fibre is a kind of aluminosillicate fibre which is mainly composed of oxides such as SiO_2, Al_2O_3, Fe_2O_3, CaO, MgO, Na_2O, K_2O, P_2O_5 and so on. X-ray diffraction indicated that the bulk structure of the fibres is non-crystal with a short range order but no long range order. SEM observation found that basalt fibre is circular in cross-section and smooth in the longitudinal direction. Solubility experiments revealed the superior resistance of the fibre to acids, alkaline and organic solvents. DGA demonstrated there are three weight loss stages in the process of elevating temperature. They are, respectively, evaporation of moisture in the fibre at about 100 °C, decomposition of the residual carbonate minerals between 480 °C and 630 °C, and decomposition of newly generated carbonates between 850~995 °C. On the heat flow curve, there are also three endothermic peaks, where the first and second correspond to the last two stages of weight loss and the third to the melting process of the fibre, whose onset is from 1122.14 °C, reaching a peak value at 1194.96 °C, and ending at 1380 °C. The tensile strength of basalt filaments and staple fibre was measured. Tensile and shear properties of the fibre were also tested.

Key words: *basalt fibre, composition, property.*

Introduction

Basalt fibre is made from a single material, crushed basalt, which is composed of the following minerals: plagioclase, pyroxene, and olivine. Essentially, no other materials are added. The basalt is simply washed and then sent to be melted down [1, 2]. The manufacture of basalt fibre requires the melting of quarried basalt rock at about 1.400 °C (2.550 °F). The molten rock is then extruded through small nozzles to produce continuous filaments of basalt fibre. The fibres typically have a filament diameter of between 9 and 13 μm, which is far enough above the respiratory limit of 5 μm to make basalt fibre a suitable replacement for asbestos [3]. They possess high thermal resistance [4, 5] as well as excellent corrosion and chemical durability [6, 7]. They also have a high elastic modulus, resulting in excellent specific tenacity – three times that of steel [8, 9]. They can be used as a fireproof textile in the aerospace and automotive industries and can also be used as a composite to produce products such as high pressure vessels (e.g. tanks and gas cylinders), load bearing profiles, windmill blades, and sports equipment. They can also be used in concrete reinforcement (e.g. for bridges and buildings) [1, 2].

Although it is similar to glass fibre in manufacturing techniques, the processing of basalt fibre is more complicated and difficult because of its high melting point. There are only a few countries that are able to manufacture continuous basalt fibre at present [2]. Thus, as a kind of recently produced fibre, basalt fibre has not been thoroughly investigated in structure and properties. In this study, the chemical composition, structure and physical and mechanical properties of basalt fibre were measured in order to clearly explain the fundamentals of the fibre and to provide the basis for further applications.

Experimental

Twist-free basalt filaments were used, produced by Dengdian Basalt Fibre Co. Ltd of Henan, China. The area of production of the basalt rock was Zhangqiu, Shandong Province, China.

The morphology of the basalt fibre was observed by JSM-6610 Scanning Electron Microscopy (JEOL Ltd., Japan). The surface of the fibre was coated with a thin conducting layer of carbon. The scanning voltage was 15 kV.

The oxides comprising the basalt fibre were quantitatively analysed by a Shimadzu Energy Dispersive X-ray Fluorescence Spectrometer – EDX-720 (Shimadzu Scientific Instruments Inc., Japan). The atmosphere was air and the collimator 10 mm.

The structure of the fibre was characterised by Shimadzu X-ray Diffractometer 7000 (Shimadzu Scientific Instruments Inc., Japan). An X-ray was emitted by a copper target when it was bombarded with fast electrons. The scanning range was 0°~80° and the scanning speed 4°/min.

Thermal properties of the fibre were analysed using a Mettler Toledo TGA/DSC1 Differential Scanning Calorimeter (Mettler Toledo, Switzerland) and Thermogravimetric Analyzer. The sample was heated from room temperature to 1300 °C in 130 minutes.

Tensile properties of the fibre were measured on an Instron 5582 (Instron Corporation, USA) for a test length of 500 mm.

Shear properties of the fibre were measured on a KES-FB1 Tensile/Shear Tester (Kato Tech Co. Ltd., Japan). Continuous filament bundles were arranged parallel to each other at a density of 10 bundles per centimetre. The samples were then preconditioned and tested at 65% and 20 °C.

Results and discussion

Scanning electron microscopy observation

There was some study by optical microscopy. The difficulty was not so much the limited resolution of the optical microscopy but the lack of depth of focus. Consequently, it could not clearly show the complex shape of a broken fibre end. SEM has great depth of focus and can give a clear three-dimensional image. It

was found by SEM observation that Basalt fibre is smooth in the longitudinal direction, like a rod [10], as shown in ***Figure 1***.

Composition analysis

Basalt rock is chemically very complex, with many different ingredients. Most of the elements existing in the earth's crust can also be found in basalt rock. And its chemical makeup varies with its place of origin. The composition of basalt fibres is directly dependent on that of the original basalt rock [1, 11]. The main compositions of the basalt rock and fibres were tested by the chemical analysis method. As a part of the elemental or oxide analysis of the mineral, loss on ignition (LOI) was also tested by strongly heating the basalt mineral at a specified temperature, allowing volatile substances to escape, until its mass ceased to change. They are listed in ***Table 1***. For the rock, the loss on ignition is roughly equivalent to the loss in mass during smelting or refining in the furnace. Similarly, the loss on ignition of the fibre indicates the extent to which the pyroprocessing was incomplete.

Then, the contents of the ingredients in the original basalt rock and fibres were determined by X-ray fluorescence spectrum analysis. They are listed in ***Table 2***. It was found that there are more than 20 oxides, such as Na_2O, MgO, Al_2O_3, SiO_2, P_2O_5, K_2O, CaO, TiO_2, Cr_2O_3, MnO, Fe_2O_3, NiO, CuO, ZnO, Rb_2O, SrO, ZrO_2, MoO_3, BaO, WO_3 et al. The contents of SiO_2, Al_2O_3, Fe_2O_3, CaO, MgO, Na_2O, K_2O and P_2O_5 are in higher amounts, accounting for 88.27% and 74.71% of the original basalt rock and fibres, respectively. While the contents of other oxides are at a lower level. Thus, the main composition of the original basalt rock and fibres are SiO_2, Al_2O_3, Fe_2O_3, CaO & MgO, which is similar to the results of chemical analysis listed in ***Table 1***.

Comparing the contents of the ingredients in the original basalt rock in ***Table 2***, it can be found that as the contents of SiO_2, Al_2O_3, MgO, Na_2O, K_2O & P_2O_5 in the fibres decrease, the contents of Fe_2O_3, CaO & MoO_3 increase, while those of the other ingredients basically remain unchanged. The major reasons for the difference may due to a sampling error, because the basalt rock may not have been of the same batch as the original basalt rock of the basalt fibres, as well as to statistical error in calculation and the difference in the loss on ignition between the original basalt rock and basalt fibres. In addition, such new ingredients as V_2O_5, Cl & Rh were added to basalt fibres in the process of spinning because of the abrasion of the spinning jet, the corrosion of machine parts at high temperature and the addition of a surface agent.

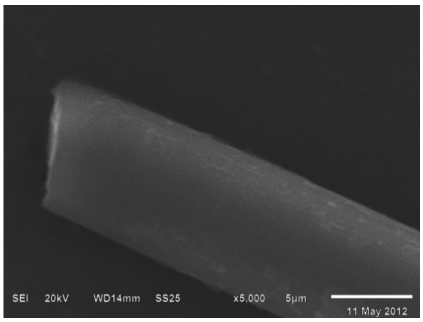

Figure 1. *Scanning electron microscopy observation of basalt fibre.*

Table 1. *Content of oxides in the basalt mineral and fibres and loss on ignition, %.*

Sample	LOI	SiO_2	Fe_2O_3	Al_2O_3	CaO	MgO
Basalt rock	1.70	54.34	9.52	13.67	6.80	5.31
Basalt fibre	0.68	50.10	6.77	14.00	2.07	5.06

Table 2. *Results of X-ray fluorescence spectrum analysis for the basalt rock and fibres.*

Molecular formula	State	Spectral line	Basalt rock			Basalt fibres		
			Net intensity	Calculated content	Statistical error, %	Net intensity	Calculated content, %	Statistical error, %
Na_2O	XRF1	Na KA1…	0.4088	3.4	6.01	0.3943	3.1	6.01
MgO	XRF1	Mg KA1…	6.020	5.37	1.42	3.843	3.31	1.81
Al_2O_3	XRF1	Al KA1-…	27.26	14.9	0.628	21.06	11.1	0.715
SiO_2	XRF1	Si KA1-…	135.9	47.46	0.280	116.2	38.96	0.303
P_2O_5	XRF1	P KA1-…	4.110	1.05	1.66	3.636	0.867	1.77
K_2O	XRF1	K KA1-…	45.36	2.418	0.487	40.14	2.119	0.518
CaO	XRF1	Ca KA1…	102.7	5.831	0.323	106.6	6.110	0.317
TiO_2	XRF1	Ti KA1-…	15.63	0.838	0.839	15.27	0.851	0.849
Cr_2O_3	XRF1	Cr KA1-…	0.5763	0.015	7.16	0.9367	0.0207	4.87
MnO	XRF1	Mn KA1…	7.908	0.120	1.27	8.553	0.139	1.22
Fe_2O_3	XRF1	Fe KA1…	678.6	7.841	0.126	736.4	9.147	0.121
NiO	XRF1	Ni KA1-…	0.7010	0.005	8.37	1.070	0.0086	5.79
CuO	XRF1	Cu KA1…	1.749	0.0096	4.14	1.926	0.0118	3.87
ZnO	XRF1	Zn KA1…	2.546	0.0110	3.30	3.030	0.0146	2.89
Rb_2O	XRF1	Rb KA1…	4.088	0.0049	3.32	3.842	0.0050	3.56
SrO	XRF1	Sr KA1-…	58.73	0.07091	0.478	61.53	0.08220	0.446
ZrO_2	XRF1	Zr KA1-…	21.21	0.0106	0.979	22.91	0.0115	0.936
MoO_3	XRF1	Mo KA1…	6.658	0.0071	2.79	161.2	0.2023	0.278
BaO	XRF1	Ba KA1-…	0.8271	0.0996	4.50	0.7798	0.107	4.68
WO_3	XRF1	W KA1-…	1.128	0.017	6.36	8.157	0.157	1.39
Cl	XRF1	Cl KA1-…				1.450	0.104	3.35
V_2O_5	XRF1	V KA1-…				1.056	0.036	10.3
Rh	XRF1	Rh KA1-…				0.1068	0.003	20.4
Content				89.43			76.39	
Computon ratio				1.12			0.942	

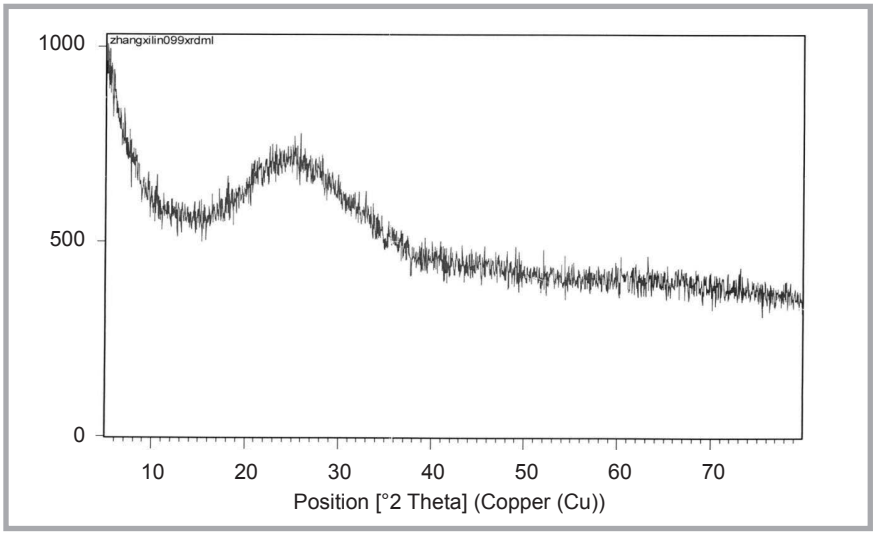

Figure 2. *X-ray diffraction spectroscopy of basalt fibre.*

The basic properties of Basalt fibre depend on its chemical composition and processing of production [3, 12]. As shown in ***Table 1*** and ***2***, basalt fibres are composed of such oxides as SiO_2, Al_2O_3, CaO, FeO, MgO et al. The fibre belongs to the aluminosillicate fibre type. As a component which makes up roughly half of the fibre, SiO_2 plays a role of network former and contributes chemical stability and excellent mechanical properties [13]. Alumina can improve the viscosity and chemical resistance of the basalt melt. The high mass ratio of Al_2O_3 gives fibre durability, chemical and thermal stability, as well as tensile properties. Na_2O, K_2O, CaO, MgO et al cannot form a network. These oxides exist in an amorphous state and take part in the structure network in the form of modifiers or transformers. Fe_2O_3 has effects on the melting parameters and thermal conductivity of basalt fibre [1]. It gives the fibre its brown colour [3].

Chemical properties

The chemical stability and durability of basalt fibres can be measured by the acidity coefficient (M_K) and pH. M_K represents the mass ratio of the main acidic oxides to the main basic oxides of which basalt fibres are composed [1]. That is

$$M_K = (W_{SiO_2} + W_{Al_2O_3})/(W_{CaO} + W_{MgO}) \quad (1)$$

where, W is the content of an oxide in the fibres. pH is also related to the content of the basic and acidic oxides as follows

$$pH = -6.2W_{SiO_2} - 12.0W_{Al_2O_3} + 23.2W_{CaO} + 12.0W_{MgO} + 14.4W_{Fe_2O_3} + 20.7W_{Na_2O} \quad (2)$$

Table 3. *Solubility of basalt fibre in different solvents.*

Solvent	Temperature, °C	Solubility
10% ~ 98% Sulfuric acid	100	insoluble
10% ~ 65% Hydrochloric acid	100	insoluble
10% ~ 68% Nitric acid	100	insoluble
30% ~ 80% Formic acid	100	insoluble
10% ~ 40% Sodium hydroxide	100	insoluble
75% Formic acid – zinc chloride	100	Insoluble
Glacial acetic acid	100	Insoluble
Phenol	100	Insoluble
Acetonitrile	100	Insoluble
Nitrobenzene	100	Insoluble
Hydrofluoric acid	25	Soluble
Dimethyl sulfoxide	100	Insoluble
Dichloromethane	100	Insoluble
5% Ethyl acetate	100	Insoluble
Carbon tetrachloride	100	Insoluble
Xylene	100	Insoluble
Pyridine	100	Insoluble
65% Potassium thiocyanate	100	Insoluble

Using the calculated contents of the constituents in ***Table 2***, the acidity coefficient M_K and pH of basalt fibre can be obtained as 5.31 and 2.61, respectively. The high acidic coefficient M_K and low pH make basalt fibres have good durability and excellent chemical stability to such solutions as salts, acids and, especially, alkalis [6, 7, 14].

The solubility of materials in a solution changes with the type and concentration of the solvent as well as with the temperature. Fibres can be identified through observing their solubility in different solvents. The solubility of basalt fibre in different solvents is listed in ***Table 3***. It can be noted that the fibre does not dissolve in such inorganic solvents as 98% sulfuric acid, 65% hydrochloric acid, 68% nitric acid, 80% formic acid, 40% sodium hydroxide, and so on, below 100 °C. It is not soluble in organic solvents such as 75% formic acid – zinc chloride, glacial acetic acid, phenol, acetonitrile, nitrobenzene et al. at a temperature of 100°C. However, basalt fibre can be dissolved in hydrofluoric acid at 25 °C.

X-ray diffraction

The X-ray diffraction pattern of a crystal is virtually a kind of sophisticated transformation of its microstructure. There is a correspondence between the structure and diffraction pattern for every crystal. Although a material may be composed of a variety of substances mixed together, the characteristic diffraction pattern for every substance does not change. The X-ray diffraction spectroscopy of basalt fibre is shown in ***Figure 2***.

It can be seen that there is no obvious diffraction peak for basalt fibre in ***Figure 2***. There is only a characteristic weak peak of typical glass state substances between 20°~30°. This indicates that basalt fibre is amorphous and there is no crystal in it. Taking the composition of the fibre into account, the bulk structure of basalt fibre resembles a chainlike skeleton mainly composed of 4 corner-sharing tetrahedral [SiO_4]. Al_2O_3 comprises part of the network structure in the form of [AlO_4], and the other oxides either fill the internal structure or are absorbed around the network. Therefore, there is a short range order but no long range order in the bulk structure of the basalt fibre [1, 11].

Thermal analysis

A TGA/DSC1 Synchronous Thermal Analyzer was able to measure the heat

flow and weight variation of the sample with the change of temperature or time. The DGA/Heatflow curve of the basalt fibre is shown in ***Figure 3***.

It can be observed there are three stages of weight loss on the DGA curve. Firstly, the weight of the fibre decreases starting from 30 °C and ending at 150 °C on the DTG curve. Obviously, this is attributed to evaporation of the moisture absorbed in the fibre. The rate of weight loss for the desorption process is -2.48%, which equals the water content of the fibre in magnitude. The second is a sharp reduction of 22.18% in the weight of the fibre between 480 °C and 630 °C, which may be attributed to the decomposition of residual carbonate minerals in the fibre. The third weight loss occurs at 850~995 °C, owing to the decomposition of newly generated carbonates [10]. The rate of weight loss is 1.06%. That is to say, the total weight loss of the fibre is only about 26% in the process of being heated from room temperature to a high temperature of 1300 °C. It can clearly be seen that the thermal stability of the fibre is very good.

There are also three endothermic peaks in the corresponding heatflow curve of the fibre. The first takes place between 514.73 °C and 620 °C, with a peak value of 578.97 °C and integral heat of 4757.67 mJ. This corresponds to the second weight loss stage on the DGA curve. The second endothermic peak on the heatflow curve begins at 661.72 °C, reaches its summit at 878.78 °C, and has an integral heat of 108.09×10^3 mJ. It corresponds to the third weight loss stage on the DGA curve of the fibre. With the rising of temperature, there is a third endothermic peak which begins from 1122.14 °C, reaches its peak value at 1194.96 °C, ends at 1380 °C, and has an integral heat of 176.62×10^3 mJ. At this stage, there is almost no weight loss in the process of elevating temperature. Hence, it indicates that the structure of the fibre is gradually destroyed and melts continuously. The fibre melts completely at 1380 °C.

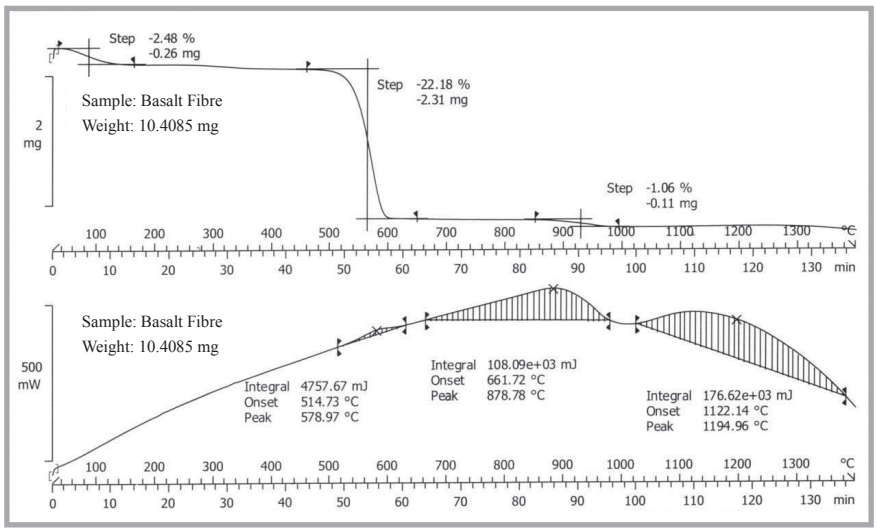

Figure 3. *DGA/Heatflow curve of the basalt fibre.*

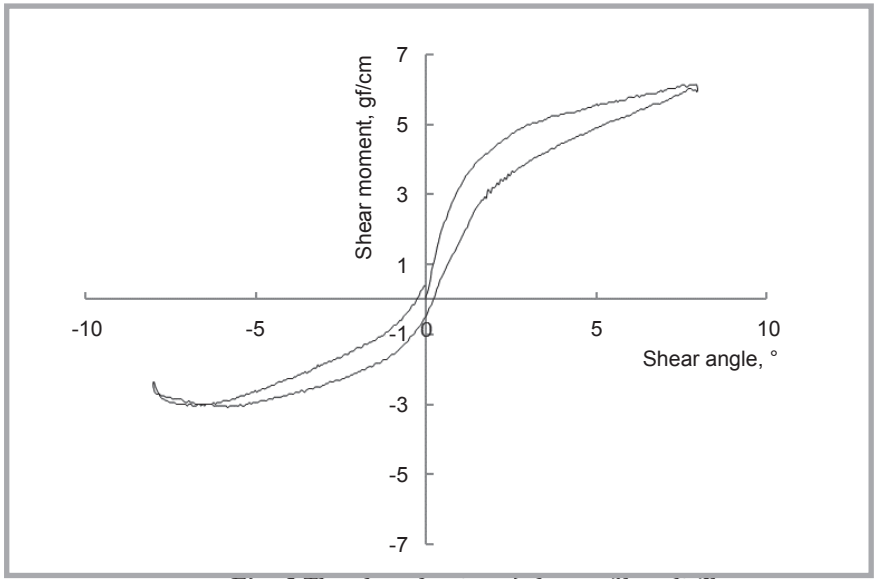

Figure 4. *Shear hysteresis loop of basalt fiber.*

Flammability

The flammability of fibres in the combustion process can be determined through observing the phenomenon occurring, the order produced, and ash left when the fibres approach the flame, are put in the flame, and after it is removed therefrom . Basalt fibre does not melt or shrink when it approaches a flame. It will curl slightly and redden like an iron wire when contacts the flame. And white smoke is given off when the fibre touches the fire. There is also a little pungent odour when burning. The fibre will stop burning when it leaves the flame. There are coke-like, crushable remains.

Tensile properties

The tensile properties of twist-free basalt filaments and staple fibres were measured. A comparison of the tensile properties of basalt filaments and staple fibres for different diameters is listed in ***Table 4***. It can be seen that basalt fibres with a smaller diameter have higher ten-

Table 4. *Tensile properties of basalt fibres.*

Parameter	Unit	Twist-free filament			Staple fibre	
Diameter	mm	9	13	18	17	22
Linear density	Tex	65	134	265	236	388
Moisture content	%	0.1	0.1	0.1	0.1	0.1
Breaking strength	MPa	2703	2231	2608	1710	2394
	N/tex	1.02	0.84	0.98	0.64	0.90
Elastic modulus	GPa	110	90	80	75.4	76
Elongation at break	%	4	3.6	3.6	2.5	3.0

Table 5. Shearing characteristics of basalt fibre.

Shear characteristics	+2HG	-2HG	2HG	+2HG5	-2HG5	2HG5	Shearing rigidity
Mean value	1.35	1.04	1.20	0.61	0.51	0.56	1.00

sile strength and elastic modulus because there are fewer bulk structure defects in fine fibres. For filaments and fibres with a similar diameter, the tensile strength and elastic modulus of basalt filaments are higher than those of staple fibres.

Shear properties

The shear properties of unidirectional basalt filaments were ascertained on a KES-FB1 Tensile/Shear Tester. The test was performed under a pretension of 10 cN/cm and maximum shear angle of ± 8°. The hysteresis curve of the basalt fibre is shown in ***Figure 4***. The shear hysteresis 2HG (0.5°) and 2HG5 (5°) as well as the shearing rigidity of basalt fibre are listed in ***Table 5***.

Conclusions

1. Basalt fibre is of the aluminosillicate fibre-type, mainly composed of oxides such as SiO_2, Al_2O_3, Fe_2O_3, CaO, MgO, Na_2O, K_2O, P_2O_5 and so on.
2. X-ray diffraction indicates that the bulk structure of the fibres is non-crystal with a short range order but no long range order.
3. The fibre has a superior resistance to most acids, alkaline and organic solvents. It is only soluble in hydrofluoric acid in the extent of the experiment.
4. Thermal analysis shows that there are stages including moisture evaporation and two decomposition process. The total weight loss in the temperature elevating process from room temperature to 1300 °C is about 26%. The melting process begins at 1122.14 °C and ends at about 1380 °C. The thermal stability of basalt fibre is excellent.

References

1. Cao Hailin, Yan Yiwu, Yue Lipei, Zhao Jinghua. *Basalt Fibers*. National Defense Industry Press, Beijing 2017: 40-57 (in Chinese).
2. Fiore V, Scalici T, Di Bella G, Valenza A. A review on basalt fibre and its composites. Composites Part B Engineering, 2015, vol. 74: 74-94.
3. Gurev VV, Neproshin EI, Mostovoi GE. The effect of basalt fiber production technology on mechanical properties of fiber. Glass and Ceramics, 2001, 58(1-2): 62-65.
4. Sarasini F, Tirillò J, Seghini MC. Influence of Thermal Conditioning on Tensile Behaviour of Single Basalt Fibres. *Composites Part B: Engineering* 2018; 132: 77-86.
5. Bhat T, Fortomaris D, Kandare E and Mouritz A P. Properties of Thermally Recycled Basalt Fibres and Basalt Fibre Composites. *Journal of Materials Science* 2018; 53(10): 1933-1944.
6. Ramachandran B E, Velpari V, Balasubramanian N. Chemical Durability Studies on Basalt Fibres. *Journal of Materials Science* 1981; 16(12): 3393-3397.
7. Wang Mingchao, Zhang Zuoguang, Li Yubin, et al. Chemical Durability and Mechanical Properties of Alkali-Proof Basalt Fiber and its Reinforced Epoxy Composites. *Journal of Reinforced Plastics and Composites* 2008; 27(4): 393-407.
8. Sokolinskaya MA , Zabava LK , Tsybulya TM, et al. Strength Properties of Basalt Fibres. *Glass and Ceramics* 1992; 49(9-10): 435-437.
9. Militký J, Kovačič V, Bajzik V. Mechanical Properties of Basalt Filaments. *FIBERS & TEXTILE in Eastern Europe* 2007, 15(5-6): 49-53.
10. Seghini M C, Pucci MF, Liotier P-J, Sarasini F, Drapier S. Surface Characterisation and Wetting Properties of Single Basalt Fibres. *Composites Part B: Engineering* 2017; 109: 72-81.
11. Lei Jing, Dang Xin'an, Zhang Hao and Li Jianjun. Analysis on Basalt Ore and Crystallization Temperature of Basalt Melt. *Journal of Shaanxi University of Science & Technology* 2007; 25(2), 63-66 (in Chinese).
12. Deák T, Czigány T. Chemical Composition and Mechanical Properties of Basalt and Glass Fibers: A Comparison. *Textile Research Journal* 2009; 79(7): 645-651.
13. Felix Bauer, Manuel Kempf, Frank Weiland, Peter Middendorf. Structure-Property Relationships of Basalt Fibers for High Performance Applications. *Composites Part B: Engineering* 2018; 145: 121-128.
14. Wei Bin, Cao Hailin, Song Shenhua. Environmental Resistance and Mechanical Performance of Basalt and Glass Fibers. *Materials Science and Engineering A* 2010; 527: 4708-4715.

Received 23.04.2018 Reviewed 20.11.2019